The $2\nu_5$ Overtone Band of Cyanoacetylene by High Resolution FTIR Spectroscopy

K. M. T. Yamada [a, b], A. Moravec [a], M. Niedenhoff [a], H. Bürger [c], and G. Winnewisser [a]

[a] I. Physikalisches Institut, Universität zu Köln, Zülpicher Str. 77, D-50937 Köln
[b] National Institute for Advanced Interdisciplinary Research (NAIR), Higashi 1-1-4, Tsukuba, Ibaraki 305, Japan
[c] Anorganische Chemie, FB 9, Bergische Universität – Gesamthochschule Wuppertal, Gaußstr. 20, D-42097 Wuppertal

Z. Naturforsch. **51a**, 27–35 (1996); received November 25, 1995

The $2\nu_5$ overtone band of cyanoacetylene, HCCCN, has been measured with a high resolution FTIR spectrometer. The analysis of the accidental resonances results in very accurate parameters for the observed $v_5 = 2$ state as well as for the hidden perturber state ($v_4 = 1$, $v_7 = 2$); the vibrational energy and the rotational constant have been determined to be 1312.991921(23) cm^{-1} and 4552.38440(23) MHz for the $v_5 = 2$ state, and 1310.0627(6) cm^{-1} and 4572.463(4) MHz for the ($v_4 = 1$, $v_7 = 2$) state. The associated hot bands from the $v_7 = 1$, $v_6 = 1$, and $v_5 = 1$ state have also been analyzed.

1. Introduction

Cyanoacetylene, HCCCN, is a molecule of great astrophysical interest, and its rotational and rovibrational spectra have been intensively investigated by high resolution spectroscopy during the last 20 years. In addition to the fairly complete laboratory spectra of this molecule and its isotopomers in the ground vibrational state in the microwave (MW) and millimeter wave (mmW) region, reported by Creswell et al. [1] and by de Zafra [2], we have recently extended the ground state measurements into the sub-millimeter wave (sub-mmW) region [3]; the accurate rotational and centrifugal distortion constants in the ground state supply very valuable information for further spectroscopic studies in the infrared region.

The MW and mmW spectra of HCCCN in some low energy excited vibrational states (lower than 1000 cm^{-1}) were studied in detail by Yamada and Creswell [4]. They measured and analyzed the pure rotational spectra of this molecule in the vibrational states of $(v_4, v_5, v_6, v_7) = (0, 0, 0, n)$ with $n = 1$ to 4, (0, 0, 1, 0), (0, 0, 1, 1), (0, 0, 1, 2), (0, 0, 2, 0), (0, 1, 0, 0), (0, 1, 0, 1), (1, 0, 0, 0) and (1, 0, 0, 1). The vibrational modes of HCCCN are listed in Table 1 together with the band center positions determined by high resolution infrared spectroscopy; the most recent papers concerning the fundamental bands are, to our knowledge, presented by Mallinson and Fayt [5] for ν_1 and ν_7, Yamada et al. [6] for ν_2, Yamada and Winnewisser [7] for ν_3, and Yamada and Bürger [8] for ν_5 and ν_6. The lowest stretching excited state, $v_4 = 1$, is strongly perturbed by a Fermi resonance with the $v_6 = 2$ state. The deperturbed band origin of ν_4 was estimated by Yamada and Creswell [4] from the analysis of anharmonic resonances.

In the present study, we have measured the rovibrational spectrum of an overtone band, $2\nu_5$, near 1300 cm^{-1} with a high resolution Fourier-transform infrared (FTIR) spectrometer. The band is extraordinarily strong for an overtone band; its intensity is comparable to that of the fundamental bands. Because of the increase of the state density in this energy region, we have detected some accidental resonances in the main band and the associated hot bands. The analysis has been carried out with the effective Hamil-

Table 1. Vibrational energies of HCCCN in cm^{-1}.

Mode		Band Origin
ν_1	CH str.	3327.372(3) [a]
ν_2	CN str.	2273.9954(3) [b]
ν_3	C≡C str.	2079.306(2) [c]
ν_4	C–C str.	884.766 [d]
ν_5	HCC bend.	663.2220(8) [e]
ν_6	CCN bend.	498.8022(12) [e]
ν_7	CCC bend.	222.402(15) [e]

[a] [5]. [b] [6]. [c] [7]. [d] Unperturbed value from [4]. [e] [8].

Reprint requests to Prof. G. Winnewisser.

0932-0784 / 96 / 0100-0027 $ 06.00 © – Verlag der Zeitschrift für Naturforschung, D-72072 Tübingen

tonian for linear molecules with two bending modes developed by Yamada and co-workers [9, 10], which has been used successfully in the analysis of the complicated spectra of triacetylene (HC_6H) [11, 12] and cyanobutadiyne (HC_5N) [13]. In order to analyze the accidental resonances observed in the spectra, which are resonances due to the quintic anharmonic potential term of k_{45577}, additional off-diagonal terms between the vibrational states have been introduced in this study. Limited information for the $v_5=2$ state from the hot band analysis of the fundamental ν_5 band was presented by Arie et al. [14].

The notation of the vibrational states and rovibrational wavefunctions in this paper follows those given [10] (see also [11–13]), with extension to three bending modes and an additional stretching vibrational mode, ν_4.

II. Observed Spectra

The measurements have been carried out in Wuppertal, using a Michelson-type high resolution FTIR spectrometer (BRUKER IFS 120). Using a cell of 278 mm optical length made of glass with KBr windows, the interferogram has been recorded for the wavenumber region from 750 to 1400 cm^{-1}, with a sample pressure of 200 Pa at room temperature. The obtained resolution was 0.0025 cm^{-1}. The observed band is fairly strong, as shown in Figure 1.

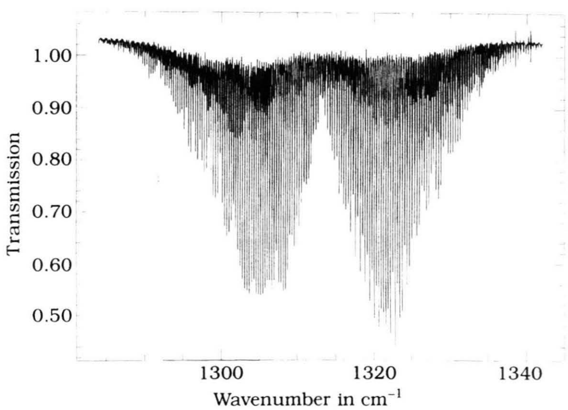

Fig. 1. The $2\nu_5$ overtone band of HCCCN measured in the present work. The transmission larger than 1 was caused by the slight difference in the optical alignments for the sample measurement and the reference (with empty cell) measurement.

The line positions were calibrated by using water lines, which were measured simultaneously because residual water remained in the evacuated spectrometer chamber with very low pressure. In the region between 1260 and 1400 cm^{-1}, 33 water lines were identified in the spectra. The water line positions listed by Guelachvili and Rao [15] were used as standard, and the linear calibration factor was obtained by a least-squares fit; the water line positions were reproduced with a standard deviation of 4.1 MHz.

A part of the observed spectrum from 1326 to 1327 cm^{-1} is reproduced in Fig. 2, showing the rotational fine structure typical for a parallel band of a polyatomic linear molecule. The strong, almost equidistant lines belong to the main series of the $2\nu_5$ band; i.e. $(v_4, v_5, v_6, v_7)^{k\pm} = (0,2,0,0)^{0\pm} \leftarrow (0,0,0,0)^{0\pm}$, where k represents the sum of the vibrational angular momenta l_i:

$$k = l_5 + l_6 + l_7 \,. \tag{1}$$

The associated doublet series, in Fig. 2, belongs to the hot band from $v_7=1$, $(0,2,0,1)^{1\pm} \leftarrow (0,0,0,1)^{1\pm}$ with resolved ℓ-type doublets, and the weak singlet series is assigned to the hot band from $v_6=1$, $(0,2,1,0)^{1\pm} \leftarrow (0,0,1,0)^{1\pm}$, with unresolved ℓ-type doublets; analyses of those bands are discussed in the following sections.

III. Analysis of the Main Band $2\nu_5$

Figure 3 shows a part of the observed spectrum where the anomalous shifts in the line positions and anomalous changes in intensities are visible for the main band as well as for the hot band from $v_7=1$. The position of the R(69) line of the $2\nu_5$ band is very close to the R(70) line, because the energy levels are shifted upwards for $J' \le 70$ and downwards for $J' \ge 71$.

The effective Hamiltonian for polyatomic linear molecules defined in [10] and used in [11–13], has been applied in the present study for describing the unperturbed energy levels; the Hamiltonian which contains the parameters for the generic ℓ-type interactions required in the present study, is

$$\hat{H} = \hat{h}_d + \hat{h}_0 + \hat{h}_2 \,, \tag{2}$$

with

$$\hat{h}_d = G_v + \sum_{i \le j} x_{L(ij)} \hat{p}_{z(i)} \hat{p}_{z(j)} + (B_v + d_{JK} \hat{J}_z^2)(\hat{J}^2 - \hat{J}_z^2) - D_v (\hat{J}^2 - \hat{J}_z^2)^2 + H_v (\hat{J}^2 - \hat{J}_z^2)^3 \,, \tag{3}$$

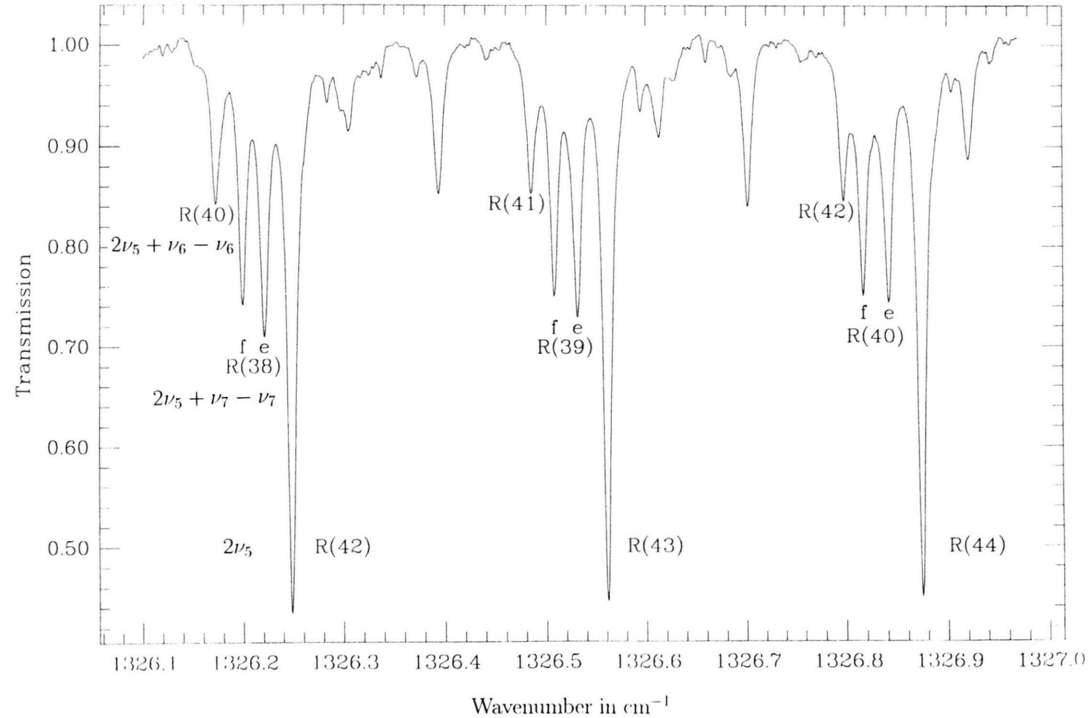

Fig. 2. A part of the observed spectrum from 1326 to 1327 cm^{-1}, showing the regular rotational fine structure. The assignments for the $2\nu_5$, $2\nu_5+\nu_7-\nu_7$, and $2\nu_5+\nu_6-\nu_6$ are indicated.

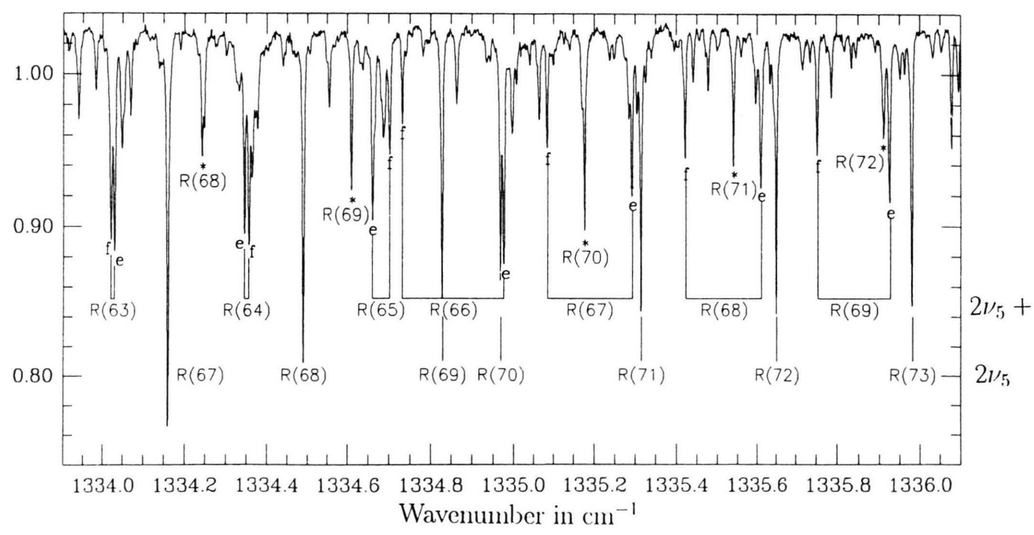

Fig. 3. A part of the observed spectrum of HCCCN showing the anomalous shifts for the transitions of the $2\nu_5$ and the $2\nu_5+\nu_7-\nu_7$ band due to the anharmonic resonances. The transitions of the $\nu_4+2\nu_7$ band, whose intensities are enhanced by the resonance, have been identified as indicated with * symbols.

$$\hat{h}_0 = \sum_{i<j} r_{ij}(\hat{L}_{++(i)}\hat{L}_{--(j)} + \hat{L}_{--(i)}\hat{L}_{++(j)}), \tag{4}$$

$$\hat{h}_2 = \frac{1}{2}\sum_i \{\hat{L}_{++(i)}\hat{J}_-(q_i + q_{Ji}\hat{J}^2)\hat{J}_- + \hat{L}_{--(i)}\hat{J}_+(q_i + q_{Ji}\hat{J}^2)\hat{J}_+\}. \tag{5}$$

Figure 4 shows the deviations of the observed line positions of the $2\nu_5$ main band from the ones calculated in the preliminary analysis using the effective Hamiltonian given above. A typical deviation pattern due to the avoided crossing of the interacting levels can be clearly seen in this figure; the interacting levels are crossing between $J = 70$ and 71. A careful look also reveals another, very small, avoided level crossing effect between $J = 28$ and 29.

Referring to the predictions of the vibrational energy levels of this molecule recently made by Fayt [16], we have assigned the perturber level to the $(1, 0, 0, 2)^{0,2}$ combination state. Thus we have introduced the following higher order anharmonic potential terms in our Hamiltonian:

$$V_1 = k_{45577}\, q_4 q_{5+} q_{5-} q_{7+} q_{7-}, \tag{6}$$

$$V_2 = \tfrac{1}{2} k'_{45577}\, q_4 (q_{5+}^2 q_{7-}^2 + q_{5-}^2 q_{7+}^2). \tag{7}$$

The first one causes a non-vanishing off-diagonal matrix element which is of present interest:

$$\langle v_4 + 1, v_5 - 2(l_5), v_6(l_6), v_7 + 2(l_7); J, k \,|\, V_1 \,|\, v_4, v_5(l_5), v_6(l_6), v_7(l_7); J, k\rangle = k_{45577}\sqrt{\frac{v_4+1}{1}}\sqrt{\frac{v_5+l_5}{2}}\sqrt{\frac{v_5-l_5}{2}} \cdot \sqrt{\frac{v_7+l_7+2}{2}}\sqrt{\frac{v_7-l_7+2}{2}} \tag{8}$$

which is, with a proper combination of quantum numbers for the present case,

$$F_1 = \langle 1, 0(0), 0(0), 2(0); J, 0 \,|\, V_1 \,|\, 0, 2(0), 0(0), 0(0); J, 0\rangle = k_{45577}/\sqrt{2}, \tag{9}$$

where the wavefunctions are represented by quantum numbers as $|v_4, v_5(l_5), v_6(l_6), v_7(l_7); J, k\rangle$. The second one, which represents an anisotropy in the potential energy surface along the molecular axis, causes

$$\langle v_4 + 1, v_5 - 2(l_5 \pm 2), v_6(l_6), v_7 + 2(l_7 \mp 2); J, k \,|\, V_2 \,|\, v_4, v_5(l_5), v_6(l_6), v_7(l_7); J, k\rangle$$

$$= \frac{1}{2} k'_{45577}\sqrt{\frac{v_4+1}{2}}\sqrt{\frac{v_5 \mp l_5}{2}}\sqrt{\frac{v_5 \mp l_5 - 2}{2}}\sqrt{\frac{v_7 \mp l_7 + 2}{2}}\sqrt{\frac{v_7 \mp l_7 + 4}{2}} \tag{10}$$

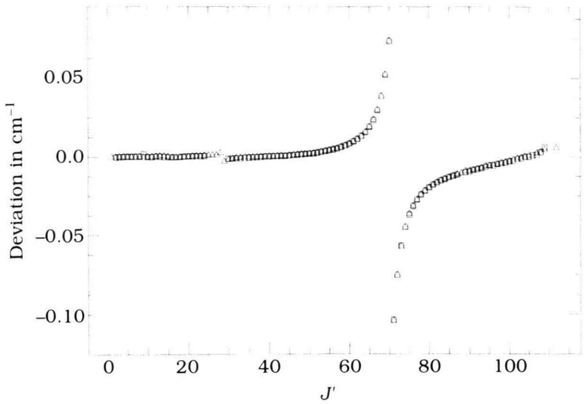

Fig. 4. The deviations of the line positions of the $2\nu_5$ band from those calculated by the effective Hamiltonian without additional perturbation terms are plotted for the upper state J quantum number. The data of the R branch are represented by the squares and of the P branch by the triangles.

with actual quantum numbers,

$$F_2 = \langle 1, 0(0), 0(0), 2(\pm 2); J, \pm 2 \,|\, V_2 \,|\, 0, 2(\pm 2), 0(0), 0(0); J, \pm 2\rangle = k'_{45577}/\sqrt{2}. \tag{11}$$

The energy eigenvalues are then calculated by diagonalizing the following energy matrix for each J:

	$\psi(2)$	$\psi(0)$	$\phi(2)$	$\phi(0)$	$\psi(-2)$	$\phi(-2)$
$\psi(2)$	$a_5(1,1)$	$a_5(1,2)$	F_2	0	$b_5(1,1)$	0
$\psi(0)$		$a_5(2,2)$	0	F_1	$a_5(1,2)$	0
$\phi(2)$			$a_7(1,1)$	$a_7(1,2)$	0	$b_7(1,1)$
$\phi(0)$				$a_7(2,2)$	0	$a_7(1,2)$
$\psi(-2)$					$a_5(1,1)$	F_2
$\psi(-2)$						$a_7(1,1)$

, (12)

where the shortened notations for the wavefunctions,

$$\psi(l_5) = |0, 2(l_5), 0(0), 0(0); J, k\rangle, \tag{13}$$

$$\phi(l_7) = |1, 0(0), 0(0), 2(l_7); J, k\rangle, \tag{14}$$

are used, and the a and b matrix elements are listed in [10, 11]. In the present analysis, the matrix given above was block diagonalized first by taking the symmetric and the antisymmetric linear combinations, and then each block was diagonalized numerically.

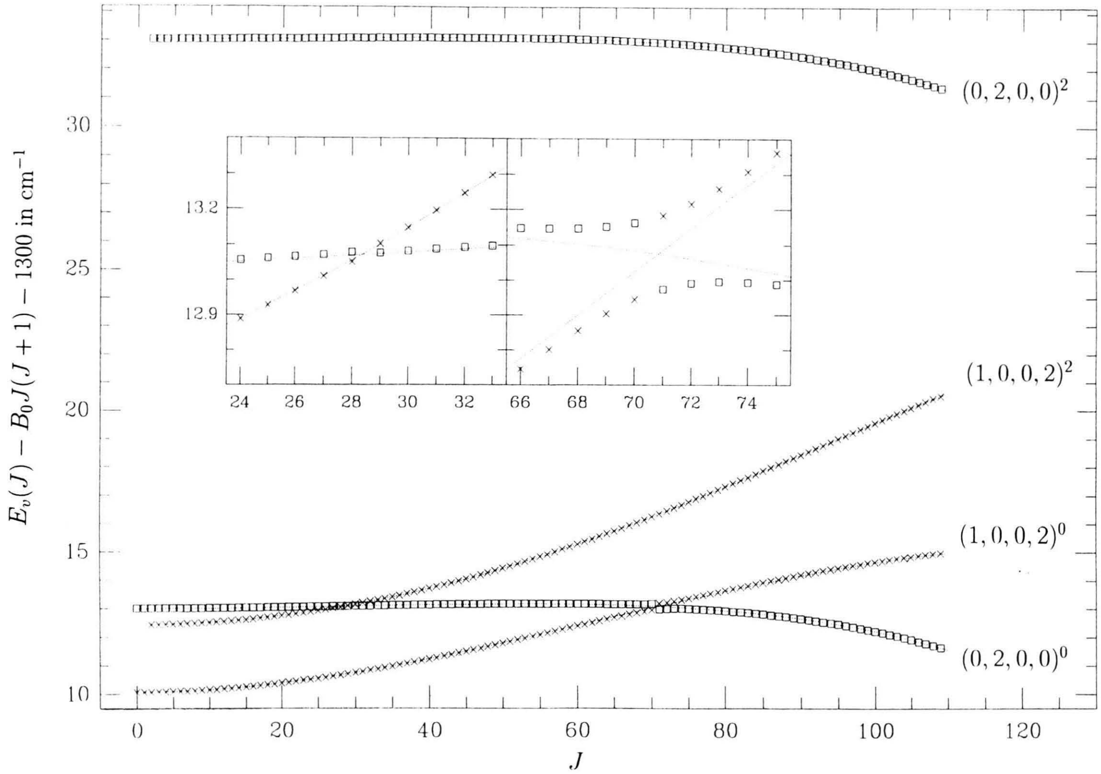

Fig. 5. The calculated energy levels of HCCCN near 1300 cm^{-1} are plotted for each J in the reduced form. The sections where the avoided level crossings have been observed are presented in an expanded scale.

The rotational and centrifugal distortion constants, the ℓ-type interaction constants, and the anharmonic interaction constants have been determined by a least-squares fitting procedure using the presently observed line positions, from P(113) to R(108), together with all available MW, mmW and sub-mmW transition in the ground vibrational state. For the $v_5=2$ state we have measured in the present work the pure rotational spectrum in the sub-mmW region from 590 GHz to 710 GHz, including the perturbed transitions. The first guess for the vibrational energy of the $\nu_4+2\nu_7$ combination state was made by using the information supplied by Prof. A. Fayt [16].

As final results, we found that the anisotropic anharmonic interaction is negligible, i.e. $F_2=0$, and we obtained rovibrational energy levels of both the $2\nu_5$ state and $\nu_4+2\nu_7$ state as illustrated in Figure 5. The unperturbed energy levels of the $(0,2,0,0)^{0+}$ state cross with those of $(1,0,0,2)^{0+}$ between $J=70$ and 71, and the levels with nearby J numbers are shifted by the anharmonic interaction F_1 as shown in the figure by an enlarged scale. The $(0,2,0,0)^{0+}$ state also crosses with the $(1,0,0,2)^{2+}$ state between $J=28$ and 29. A very weak anharmonic resonance between these two states is induced by the mixing of the wavefunctions of the $\ell=0$ and 2 components due to the ℓ-type resonance interaction in the $(1,0,0,2)$ state. This resonance also causes an avoided crossing effect, and the corresponding shifts in the line positions have been observed as shown in Fig. 4 although they are very small.

The best fit parameters obtained in the present analysis are listed in Table 2. The parameters x_{L55} and d_{JL} of the $v_5=2$ state are fixed at the value derived from the $2\nu_5-\nu_5$ hot band analysis by Arie et al. [14]. Several parameters for the hidden state, $(1,0,0,2)$, have been fixed at the value estimated from the $v_7=2$ state. The fit is quite satisfactory; almost all residuals of the fit are smaller than ± 0.0005 cm^{-1} for the infrared transitions, which is the present experimental uncertainty. The sub-mmW transitions have been fitted well except the lines very close to the

Table 2. Parameters determined for the $2\nu_5$ band of HCCCN.

Parameter	Unit	(0, 0, 0, 0)	(0, 2, 0, 0)	(1, 0, 0, 2)
G_v	cm^{-1}		1312.991921 (23)	1310.0627 (6)
x_{L55}	cm^{-1}		5.16 (*fix*) [a]	
x_{L77}	cm^{-1}			0.74221 (28)
B_v	MHz	4549.05838 (7)	4552.38440 (23)	4572.463 (4)
d_{JL}	kHz		−240.0 (*fix*) [a]	−14.0 (*fix*) [b]
D_v	Hz	544.13 (3)	547.99 (8)	593.0 (*fix*) [b]
H_v	mHz	0.035 (3)	0.054 (7)	0.024 (*fix*) [b]
q_5	MHz		2.5374 (*fix*) [b]	
q_7	MHz			6.8 (*fix*) [b]
q_{J7}	Hz			−40.0 (*fix*) [b]
k_{45577}	cm^{-1}		0.159243 (23)	

[a] Derived from [14]. [b] From [4].

avoided crossing; the observed R(69) transition frequency is off from the calculated value by about −1 MHz, and the R(70) by 3 MHz. It was not possible to further improve the fit, which may be limited by the effective Hamiltonian used in the present analysis. The parameters obtained for the ground state are essentially determined by the MW, mmW, and submmW data, and are consistent with our previous values [3].

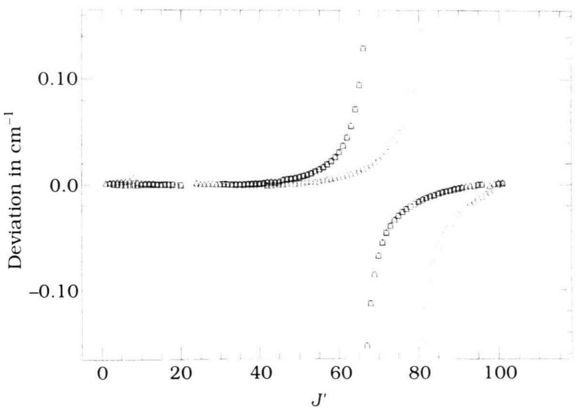

Fig. 6. The deviations of the line positions of the $2\nu_5+\nu_7-\nu_7$ band from those calculated by the effective Hamiltonian without additional perturbation terms are plotted for the upper state J quantum number. The data of R branch are represented by squares (□) and of P branch by triangles (△); the levels of f symmetry by solid, and of e symmetry by broken symbols. Because of the ℓ-type doubling effect, the crossing points are different for the two components of the ℓ-type doublet.

IV. Analysis of the Hot Bands

The hot band $2\nu_5+\nu_7-\nu_7$

A similar anharmonic resonance was observed in an associated hot band from the $v_7=1$ state, $(0,2,0,1)^{1\pm} \leftarrow (0,0,0,1)^{1\pm}$. The ℓ-component with the superscript "+", the symmetric linear combination, is of f state, and "−", the antisymmetric linear combination is of e state in this case. The observed anomalies are illustrated in Fig. 6, where the e and f components cross the perturber levels at different J because of the large ℓ-type doubling splitting. In Fig. 3 the anomalous line shifts of the f lines are visible; the maximum upward shift is observed for R(65) and the downward shift for R(66).

The perturber state is, as a natural consequence, the state with one quantum higher in v_7 than in the case of the resonance found in the main band, i.e. $(1,0,0,3)^{1\pm}$.

A non-vanishing matrix element caused by the anharmonic potential V_1 of (6) is, in the present case,

$$F_1' = \langle 1,0(0),0(0),3(\pm 1); J, \pm 1 | V_1 | 0,2(0),0(0),1(\pm 1); J, \pm 1\rangle = k_{45577}, \tag{15}$$

and by the anisotropic potential V_2 in (7),

$$F_2' = \langle 1,0(0),0(0),3(\pm 1); J, \pm 1 | V_2 | 0,2(\pm 2),0(0),1(\mp 1); J, \pm 1\rangle = k'_{45577}/\sqrt{2}. \tag{16}$$

The V_2 causes also an interaction for the $k=3$ state as

$$F_2'' = \langle 1,0(0),0(0),3(\pm 3); J, \pm 3 | V_2 | 0,2(\pm 2),0(0),1(\pm 1); J, \pm 3\rangle = k'_{45577}/\sqrt{2}. \tag{17}$$

The energy matrix to be diagonalized is of dimension 10×10 in this case, and by ordering the basis wavefunctions with the sign of k, we can make its form to be

$$\begin{array}{|c|c|} \hline \mathbf{A} & \mathbf{B} \\ \hline \mathbf{B} & \mathbf{A} \\ \hline \end{array}, \tag{18}$$

where the matrix A is of the matrix elements between the states with k of same sign, and B of the elements between the states with k of different sign. Using the basis functions of

$$\psi(l_5, l_7) = |0, 2(l_5), 0(0), 1(l_7); J, k\rangle, \tag{19}$$

$$\phi(l_7) = |1, 0(0), 0(0), 3(l_7); J, k\rangle \tag{20}$$

the A matrix for a given J, with positive k, is

	$\psi(2,1)$	$\psi(2,-1)$	$\psi(0,1)$	$\phi(3)$	$\phi(1)$
$\psi(2,1)$	$a_5(1,1)$	$a_5(1,2)$	$a_5(1,3)$	F_2''	0
$\psi(2,-1)$		$a_5(2,2)$	$a_5(2,3)$	0	F_2'
$\psi(0,1)$			$a_5(3,3)$	0	F_1'
$\phi(3)$				$a_7(1,1)$	$a_7(1,2)$
$\phi(1)$					$a_7(2,2)$

(21)

and has the same form for negative k. The B matrix is given as

	$\psi(-2,-1)$	$\psi(-2,1)$	$\psi(0,-1)$	$\phi(-3)$	$\phi(-1)$
$\psi(2,1)$	$b_5(1,1)$	$b_5(1,2)$	$b_5(1,3)$	0	0
$\psi(2,-1)$		$b_5(2,2)$	$b_5(2,3)$	0	0
$\psi(0,1)$			$b_5(3,3)$	0	0
$\phi(3)$				$b_7(1,1)$	$b_7(1,2)$
$\phi(1)$					$b_7(2,2)$

. (22)

The energy matrix, (18), was block diagonalized by using the symmetric and antisymmetric combinations of the positive and negative k functions as a new basis,

$$\begin{array}{|c|c|} \hline A+B & 0 \\ \hline 0 & A-B \\ \hline \end{array}, \tag{23}$$

and each block was diagonalized numerically.

The observed line positions, from P(103) to R(102) of the band, have been analyzed by a least-squares fitting procedure, in a similar way as in the case of the main band together with available MW, mmW, and sub-mmW data. The contributions from the anisotropic part of the anharmonic potential, F_2' and F_2'', are found again to be negligible. The results of the final fit are listed in Table 3. The fit is not so good as in the case of the main band; there are systematic deviations of the calculated line positions from the observed ones in the range of ± 0.004 cm^{-1}. Many of the parameters were kept fixed in the fitting procedure at the estimated values as listed in Table 3. The lack of information for the hidden state (1, 0, 0, 3) did not allow us a further improvement of the fit.

The hot band $2\nu_5+\nu_6-\nu_6$

No significant resonance was visible in the observed spectra of this hot band. The standard procedures for analyzing the linear molecule spectra with two bending modes [12–14] were applied to the present data, from P(89) to R(91), and the available pure rotational data for the lower state. The sub-mmW transitions of the lower state, $v_6=1$, have been measured in the present study in the range form R(62) to R(77), which corresponds to the frequency range from 570 GHz to 710 GHz. The parameters have been determined as listed in Table 4.

Table 3. Parameters determined for the $2\nu_5+\nu_7-\nu_7$ band of HCCCN.

Parameter	Unit	(0, 0, 0, 1)	(0, 2, 0, 1)	(1, 0, 0, 3)
ΔG_v	cm^{-1}		1314.23951(16)	1309.29(5)
x_{L55}	cm^{-1}		5.16(*fix*)	
x_{L57}	cm^{-1}		0.65(*fix*)	
x_{L77}	cm^{-1}			0.71(*fix*)[a]
B_v	MHz	4563.5129(*fix*)[a]	4565.6385(28)	4591.8(3)
d_{JL}	kHz		−240.0(*fix*)	−14.0(*fix*)[a]
D_v	Hz	567.5(*fix*)[a]	525.8(3)	720.0(*fix*)
H_v	mHz	0.13(*fix*)	0.13(*fix*)	0.13(*fix*)
q_5	MHz		2.5374(*fix*)	
q_7	MHz	6.5383(*fix*)[a]	5.879(4)	6.60(9)
q_{J7}	Hz	−15.8(*fix*)	11.6(5)	109(14)
r_{57}	cm^{-1}		0.24(*fix*)	
k_{45577}	cm^{-1}		0.1737(8)	

[a] From [4].

Table 4. Parameters determined for the $2\nu_5+\nu_6-\nu_6$ band of HCCCN.

Parameter	Unit	(0, 0, 1, 0)	(0, 2, 1, 0)
ΔG_v	cm^{-1}		1313.53147(17)
x_{L55}	cm^{-1}		5.16(*fix*)
B_v	MHz	4558.3140(3)	4561.889(5)
d_{JL}	kHz		−240.0(*fix*)
D_v	Hz	554.35(9)	561.9(17)
H_v	mHz	0.052(9)	0.40(15)
q_5	MHz		2.5374(*fix*)
q_6	MHz	3.5823(4)	3.5823(*fix*)
q_{J6}	Hz	−2.08(4)	−2.08(*fix*)
r_{56}	cm^{-1}		0.3218(21)

The hot band $3\nu_5-\nu_5$

Although it is known that the $v_5=1$ state is weakly perturbed by the $v_7=3$ state through an anharmonic potential [4],

$$V_3 = \frac{1}{2} k_{5777} (q_{5+}\, q_{7-} + q_{5-}\, q_{7+})\, q_{7+}\, q_{7-}\,, \tag{24}$$

the observed infrared spectrum does not indicate any visible perturbation in this hot band. Thus in the present analysis we took only the perturbation in the lower state into account. The anharmonic potential V_3 in (24) gives a non-vanishing matrix element of

$$\begin{aligned} &\langle v_4, v_5+1(l_5 \pm 1), v_6(l_6), v_7-3(l_7 \mp 1);\\ &J, k \,|\, V_3 \,|\, v_4, v_5(l_5), v_6(l_6), v_7(l_7);\, J, k\rangle \\ &= \frac{1}{2} k_{5777} \sqrt{\frac{v_5 \pm l_5 + 2}{2}} \sqrt{\frac{v_7 + l_7}{2}} \sqrt{\frac{v_7 - l_7}{2}} \\ &\cdot \sqrt{\frac{v_7 \pm l_7 - 2}{2}}, \end{aligned} \tag{25}$$

which is, with a proper combination of quantum numbers for the present case,

$$\begin{aligned} F_3 = &\langle 0, 1(\pm 1), 0(0), 0(0);\\ &J, \pm 1 \,|\, V_3 \,|\, 0, 0(0), 0(0), 3(\pm 1);\\ &J, \pm 1\rangle = k_{5777}/\sqrt{2}. \end{aligned} \tag{26}$$

The energy matrix to be diagonalized for the lower state is of 6×6 dimension, which has a form as (18) for the $v_7 = 1$ hot band given above. Using the basis functions of

$$\psi(l_5) = |0, 1(l_5), 0(0), 0(0);\, J, k\rangle, \tag{27}$$

$$\phi(l_7) = |0, 0(0), 0(0), 3(l_7);\, J, k\rangle, \tag{28}$$

the A matrix for a given J with positive k is in this case

	$\psi(1)$	$\phi(3)$	$\phi(1)$
$\psi(1)$	$a_5(1,1)$	0	F_3
$\phi(3)$		$a_7(1,1)$	$a_7(1,2)$
$\phi(1)$			$a_7(2,2)$

, (29)

and the B matrix for negative k is

	$\psi(-1)$	$\phi(-3)$	$\phi(-1)$
$\psi(1)$	$b_5(1,1)$	0	0
$\phi(3)$	0	$b_7(1,1)$	$b_7(1,2)$
$\phi(1)$	0	$b_7(1,2)$	$b_7(2,2)$

. (30)

As in the case of the $v_7 = 1$ hot band, the energy matrix is then block diagonalized to the symmetric and antisymmetric state, (23), and then numerically diagonalized. This analysis is essentially the same as that presented in [4]. Table 5 lists the parameters obtained by the present analysis using the infrared data of P(92) to R(71), and the available mmW data for the lower states [4].

Table 5. Parameters determined for the $3\nu_5 - \nu_5$ band of HCCCN.

Parameter	Unit	(0, 1, 0, 0)	(0, 2, 0, 0)	(1, 0, 0, 2)
ΔG_v	cm^{-1}		−0.180(16)	1301.44908(8)
x_{L55}	cm^{-1}			5.16 (*fix*)
x_{L77}	cm^{-1}		0.7174(20)	
B_v	MHz	4550.6290(25)	4592.3795(29)	4553.9550(25)
d_{JL}	kHz		−13.4(3)	
D_v	Hz	548.2(13)	618.2(9)	556.8(13)
q_5	MHz	2.5381(4)		2.5863(3)
q_7	MHz		6.5885(5)	
q_{J7}	Hz		−18.3(6)	
k_{5777}	cm^{-1}	0.0500(15)		

VII. Discussion

The present work revealed the accidental resonances which cause very large shifts in the line positions. Such resonances are expected to be observed in the high vibrational energy states, because the density of states becomes so high that the accidental crossing of the interacting rovibrational levels is very probable. Resonances make the assignment and the analysis of the spectra difficult on one hand. However, if the spectra are assigned, the proper analysis of the resonance gives valuable information for the hidden pertuber states. In the present study the vibrational energy and the rotational constant of the (1, 0, 0, 2) state and of the (1, 0, 0, 3) state have been determined very accurately without observing the transitions pertaining to these high quantum number states.

In fact, some of the resonance induced transitions from the ground state to the $(1,0,0,2)^{0+}$ state have been identified in the final stage of the present work; from P(69) to P(73) and from R(66) to R(71). Since the mixing ratio of the wave-functions is very close to 50:50 near the energy crossing point, $J' \approx 70$, they are very strong, as shown in Figure 3. Corresponding intensity decreases can be clearly observed for the lines of $2\nu_5$. The intensity anomalies are also observed in the hot band $2\nu_5 + \nu_7 - \nu_7$, as shown in Figure 3. The corresponding transitions of the perturber state have, however, not been identified yet.

The list of the infrared line positions and the newly measured sub-mmW line frequencies are available from the authors upon request and will be deposited at the office of Sektion für Spektren- und Strukturdokumentation, Universität Ulm, Germany.

The authors are greatful to Dr. S. P. Belov and Dr. M. Lietdke for their help in the sub-mmW measurements, and to Prof. A. Fayt, who made the results obtained in his laboratory available to us prior to publication. The present work is supported in part by Deutsche Forschungsgemeinschaft via Research Grant SFB-301.

[1] R. A. Creswell, G. Winnewisser, and M. C. L. Gerry, J. Mol. Spectrosc. **65,** 420 (1977).
[2] R. L. de Zafra, Astrophys. J. **170,** 165 (1971).
[3] K. M. T. Yamada, A. Moravec, and G. Winnewisser, Z. Naturforsch. **50 a,** 1179 (1995).
[4] K. M. T. Yamada and R. A. Creswell, J. Mol. Spectrosc. **116,** 384 (1986).
[5] P. D. Mallinson and A. Fayt, Mol. Phys. **32,** 473 (1976).
[6] K. Yamada, R. Best, and G. Winnewisser, Z. Naturforsch. **38 a,** 1296 (1984).
[7] K. Yamada and G. Winnewisser, Z. Naturforsch. **36 a,** 23 (1981).
[8] K. M. T. Yamada and H. Bürger, Z. Naturforsch. **41 a,** 1021 (1986).
[9] K. M. T. Yamada, R. W. Birss, and M. R. Aliev, J. Mol. Spectrosc. **112,** 347 (1985).
[10] M. Niedenhoff and K. M. T. Yamada, J. Mol. Spectrosc. **157,** 182 (1993).
[11] S. Haas, K. M. T. Yamada, and G. Winnewisser, J. Mol. Spectrosc. **164,** 455 (1994).
[12] S. Haas, G. Winnewisser, K. M. T. Yamada, K. Matsumura, and K. Kawaguchi, J. Mol. Spectrosc. **167,** 176 (1994).
[13] S. Haas, G. Winnewisser, and K. M. T. Yamada, Can. J. Phys. **72,** 1165 (1994).
[14] E. Arie, M. Dang Nhu, Ph. Arcas, G. Graner, H. Bürger, G. Pawelke, M. Khlifi, and F. Raulin, J. Mol. Spectrosc. **143,** 318 (1990).
[15] G. Guelachvili and K. Narahari Rao, Handbook of Infrared Standards, Academic Press, Boston 1986.
[16] A. Fayt, private communication.